JACS JOURNAL OF THE AMERICAN CHEMICAL SOCIETY

Communication

Cite This: J. Am. Chem. Soc. 2019, 141, 18949−18953

pubs.acs.org/JACS

Selective Separation of Polyaromatic Hydrocarbons by Phase Transfer of Coordination Cages

Dawei Zhang, Tanya K. Ronson, Roy Lavendomme, and Jonathan R. Nitschke*

Department of Chemistry, University of Cambridge, Lensfield Road, Cambridge, CB2 1EW, United Kingdom

Supporting Information

ABSTRACT: Here we report a new supramolecular strategy for the selective separation of specific polycyclic aromatic hydrocarbons (PAHs) from mixtures. The use of a triethylene glycol-functionalized formylpyridine subcomponent allowed the construction of an $Fe^{II}_4L_4$ tetrahedron **1** that was capable of transferring between water and nitromethane layers, driven by anion metathesis. Cage **1** selectively encapsulated coronene from among a mixture of eight different types of PAHs in nitromethane, bringing it into a new nitromethane phase by transiting through an intermediate water phase. The bound coronene was released from **1** upon addition of benzene, and both the cage and the purified coronene could be separated via further phase separation.

Polycyclic aromatic hydrocarbons (PAHs), also known as polyaromatic hydrocarbons,[1] are found naturally in oil, coal, and tar, and they are produced as byproducts in the combustion processes of fuels. They are widespread pollutants, with many known to be carcinogenic, mutagenic, and teratogenic.[2] Their rigid, planar, conjugated structures render them useful in the fabrication of optical and electronic devices.[3,4] Both the value of PAHs in pure form, and the problems they cause as pollutants, thus motivate the development of new host molecules[5−15] for selective PAH sequestration.[16−22]

New supramolecular strategies for the separation of target molecules, based on host−guest chemistry, are of current interest.[23,24] For instance, nonporous adaptive crystals of pillararenes have been successfully employed for the separation of various aromatic and aliphatic hydrocarbons.[25,26] Porous organic cages have also been developed for the selective separation of xylene isomers,[27] noble gases,[28] and chiral molecules.[28] Our group has recently focused on the use of phase transfer[29−35] of coordination cages[36−48] and their molecular cargoes as a new strategy aiming to address practical separation problems.[49]

We have demonstrated that anion metathesis could be used to drive cages and their cargoes between phases.[50] In addition, cages that incorporate hydrophobic ligands, and which thus cannot be prepared directly in water, may in certain cases be rendered water-soluble by adding hydrophilic anions.[51] Cages constructed from large, hydrophobic aromatic panels, however, tend to decompose in water, as the equilibria of their formation are driven backward by ligand insolubility.[51]

This work describes a new method to enable the use in water of coordination cages that contain large, hydrophobic subcomponents. Coordination cage **1** (Scheme 1), constructed from a water-insoluble triazatruxene panel, is water-stable as a result of the incorporation of triethylene glycol moieties in its formylpyridine subcomponents. Cage **1** thus undergoes anion-metathesis-driven phase transfer, which in turn allows the selective separation and recovery of coronene from a mixture of similar PAHs. We also developed a means to recycle **1** by separating it from its purified coronene cargo.

Scheme 1. Subcomponent Self-Assembly of Cage 1

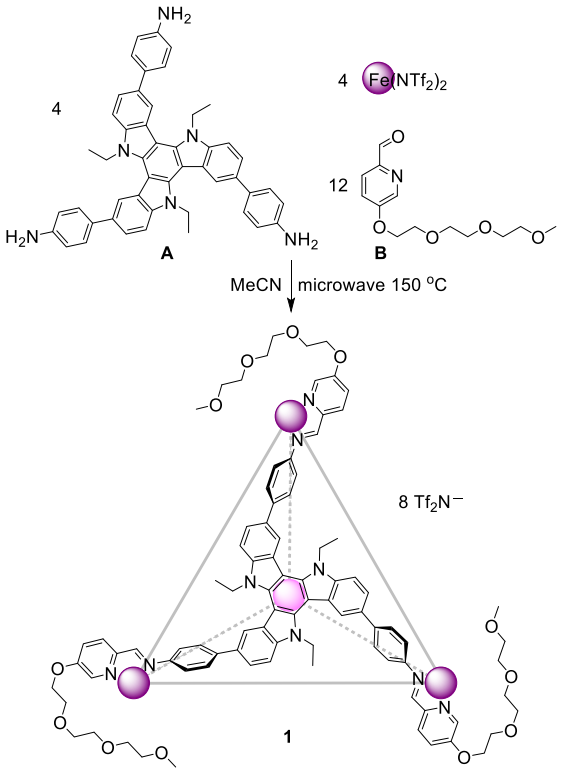

The reaction of tritopic subcomponent **A** (4 equiv) with iron(II) bis(trifluoromethanesulfonyl)imide (triflimide, Tf_2N^-) (4 equiv) and triethylene glycol-functionalized formylpyridine **B** (12 equiv) in acetonitrile afforded tetrahedron **1** (Scheme 1). The $Fe^{II}_4L_4$ composition of the assembly

Received: October 6, 2019
Published: November 15, 2019

DOI: 10.1021/jacs.9b10741
J. Am. Chem. Soc. 2019, 141, 18949−18953

was confirmed by electrospray ionization mass spectrometry (ESI-MS) (Figure S17). The ^{1}H NMR spectrum of **1** displayed only one set of ligand signals (Figure S14), consistent with the exclusive formation of a pair of *T*-symmetric tetrahedral enantiomers, with faces and vertices of a single stereochemical orientation. We infer these enantiomers to be $A_4\Delta_4$-**1** and $C_4\Lambda_4$-**1**, with anticlockwise (A) triazatruxene panels paired with iron(II) stereocenters of Δ handedness, and clockwise (C) triazatruxene with Λ-iron(II) (Figure S18a), based upon the configuration of the parent $Fe^{II}{}_4L_4$ cage (Figure S18b), without triethylene glycol groups.[52]

The gradual addition of coronene (Figure 1) to a solution of **1** (0.13 mM, 500 μL) in CD_3NO_2 led to the formation of the

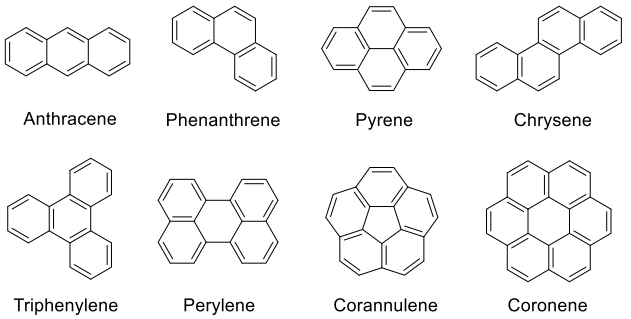

Figure 1. PAH guests for **1**.

host–guest complex coronene⊂**1**. Encapsulation was signaled by the disappearance of the ^{1}H NMR peaks of free **1** and the concurrent appearance of a new set of host peaks and a single peak for bound coronene, which was shifted upfield ($\Delta\delta$ = −1.89 ppm), consistent with a slow-exchange binding process (Figures 2 and S19). When excess coronene (3.4 equiv) was added to **1**, 85% conversion to coronene⊂**1** was observed. The degree of host–guest complexation was limited by the poor solubility (ca. 0.44 mM) of coronene in this solvent. The

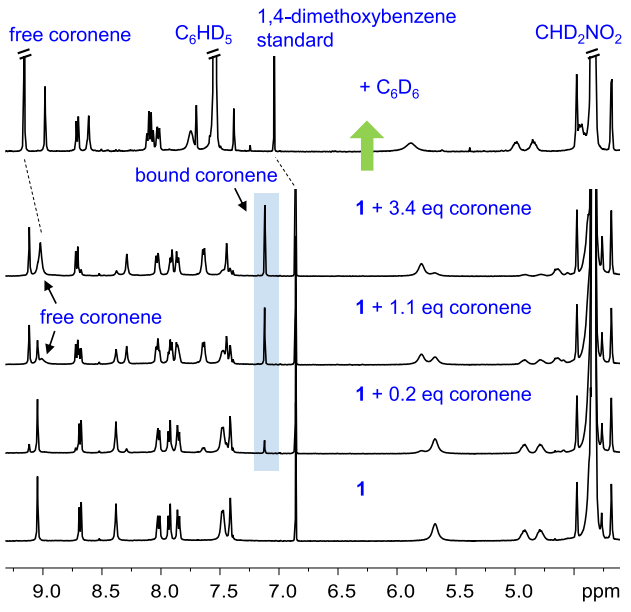

Figure 2. Partial ^{1}H NMR spectra (CD_3NO_2, 500 MHz, 25 °C) of **1** (0.13 mM) after the addition of increasing amounts of coronene and then following further addition of deuterated benzene (100 μL to a 500 μL sample) to the mixture.

bound coronene was released from the cavity of **1** upon addition of excess C_6D_6 (100 μL) (Figure 2). We infer that the coronene guest is better solvated by a solvent mixture that contains benzene, thus favoring guest release upon benzene addition.

A binding constant K_{a1} = (1.9 ± 0.3) × 10^4 M^{-1} of **1** for coronene was determined by ^{1}H NMR integration at 25 °C. The binding affinity was observed to decrease as the temperature increased (Table S1 and Figure S20). A van't Hoff analysis (Figure S21) revealed that the binding is driven by enthalpy (ΔH = −27 kJ mol^{-1}; ΔS = −1.7 × 10^{-3} kJ K^{-1} mol^{-1}).

Decreasing the concentration of **1** to 0.040 mM allowed us to add 10 equiv of coronene without precipitation. In this experiment a new singlet peak, corresponding to the bound coronene of a 1:2 host–guest complex, was also observed (Figure S22), as assigned using NOESY and HSQC spectra (Figures S24 and S25). A binding constant of K_{a2} = (1.1 ± 0.2) × 10^3 M^{-1} was determined from integration. The affinity of **1** for a second coronene is thus more than an order of magnitude less than for the first (1.9 × 10^4 M^{-1}). PM3 models (Figure S23) indicate room for two molecules of coronene within **1** without distortion.

Addition of other PAH guests, such as anthracene, phenanthrene, pyrene, chrysene, triphenylene, and perylene, resulted in gradual shifts of the peaks of **1** as well as the guests, consistent with fast-exchange binding on the NMR chemical shift time scale (Figures S26–S31). Binding constants were not determined in these cases due to the low solubilities of the guests and host–guest peak overlaps. Similarly to coronene, corannulene was observed to bind in slow exchange (Figures S32–S34), but the binding strength ((2.8 ± 0.4) × 10^3 M^{-1}) was 7 times weaker than for coronene. We infer the high selectivity of the cage toward coronene to result from a better size match with the inner cavity, as compared to the other, smaller, guests.[17]

We tested the phase transfer of free **1** between two liquid phases, namely, D_2O and CD_3NO_2, triggered by anion exchange.[50] The assembled cage with triflimide counteranions was initially soluble in the lower nitromethane layer, transferring to the upper water layer after addition of tetrabutylammonium sulfate (8 equiv) as anion exchange took place (Figures 3 and S35–S37). Removal and replacement of the nitromethane layer with fresh nitromethane, followed by addition of lithium triflimide (16 equiv), led **1** to transfer back into the new nitromethane layer, as signaled by the deep red color of **1**.

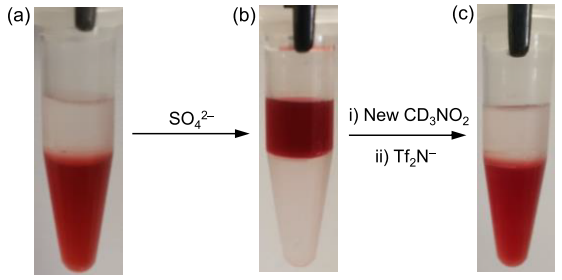

Figure 3. Sequential phase transfer of **1** (0.13 mM) by addition of sulfate and triflimide anions, from CD_3NO_2 (lower layers) to D_2O (upper layers) and back again.

DOI: 10.1021/jacs.9b10741
J. Am. Chem. Soc. 2019, 141, 18949–18953

The ^{1}H NMR spectra of **1** in the initial and final CD_3NO_2 phases presented well-defined cage peaks, the integrations of which suggested that more than 95% of **1** transferred through water and back into nitromethane (Figure S35). The proton signals of **1** in the intermediate D_2O phase were broad but became sharper after the addition of acetone-d_6 (Figure S36), consistent with *T* point symmetry. This tetrahedron paired with sulfate was also detected by ESI-MS (Figure S37). We infer that the cage molecules tend to aggregate in water, giving rise to broad ^{1}H NMR signals, while dispersion occurs after addition of a water-miscible organic solvent.[53]

Notably, an analogue of **1** having no peripheral triethylene glycol groups (Figure S18b) was not observed to transfer into water, even following the addition of a large excess (>100 equiv) of sulfate. Instead it decomposed to produce insoluble solids, demonstrating the necessity of incorporating hydrophilic triethylene glycol groups into subcomponent **B**.

We then set about investigating the use of cage **1** to build a system capable of chemical purification by catching and releasing a coronene cargo. As shown in Figure S38, the addition of sulfate (8 equiv) to a mixture of **1** (0.090 mM, 500 μL) and coronene (3.7 equiv) led to the transfer of the cage with its cargo into the D_2O layer (Figure S38b). Subsequent addition of triflimide (16 equiv) drove the complex back to a new CD_3NO_2 layer (Figure S38c). The bound coronene was released from **1** following the addition of C_6D_6 (100 μL, Figure S38d). The ^{1}H NMR spectrum of this solution indicated the presence of free **1** and free coronene (0.86 equiv, Figure S39), without host–guest complex peaks. Replacement of the upper D_2O layer and addition of sulfate (8 equiv) resulted in transfer of the free cage to the new D_2O layer. The coronene was thus isolated through evaporation of the CD_3NO_2 (Figure S38e). Cage **1** was recovered as the triflimide salt in fresh nitromethane after a final anion metathesis step (Figure S38f).

Intriguingly, an aqueous solution of **1** as the sulfate salt (Figure S38e) could be also used for direct extraction of coronene from CD_3NO_2 (Figure S40), with comparable efficiency to the procedure involving phase transfer. The combination of extraction and subsequent phase transfer thus offers an alternative route to coronene separation and recycling.

Cage **1** was able to selectively separate coronene from a mixture of other PAHs including anthracene, phenanthrene, pyrene, chrysene, triphenylene, perylene, and corannulene (Figure 4). A similar sequential phase-transfer process as described above was performed, resulting in the successful separation of the coronene target from the other PAHs. The coronene (0.75 equiv) was isolated in CD_3NO_2, with no other PAHs detectable by ^{1}H NMR (Figure S42), indicating a high selectivity. The amount of coronene isolated (0.75 equiv) was slightly less than the amount obtained (0.86 equiv) when no other PAHs were present. Control experiments showed that, when the mixture of PAHs contained only these other guests without coronene, no PAH molecules were transported during phase transfer of **1** (Figure S43). This observation suggests that the weaker interactions of these other PAHs with **1** led to their ejection during phase transfer. However, their presence appeared to slightly decrease the coronene transport efficiency, which we infer to be a consequence of their blocking the cavity of **1**.

The triethylene glycol functionalization strategy developed herein may well allow other cages to undergo phase transfer, in turn permitting the purification of a wider range of molecules.[54] This method may thus be rendered useful in the purification of valued products from many different sources, from petroleum feedstocks to drug synthesis procedures.

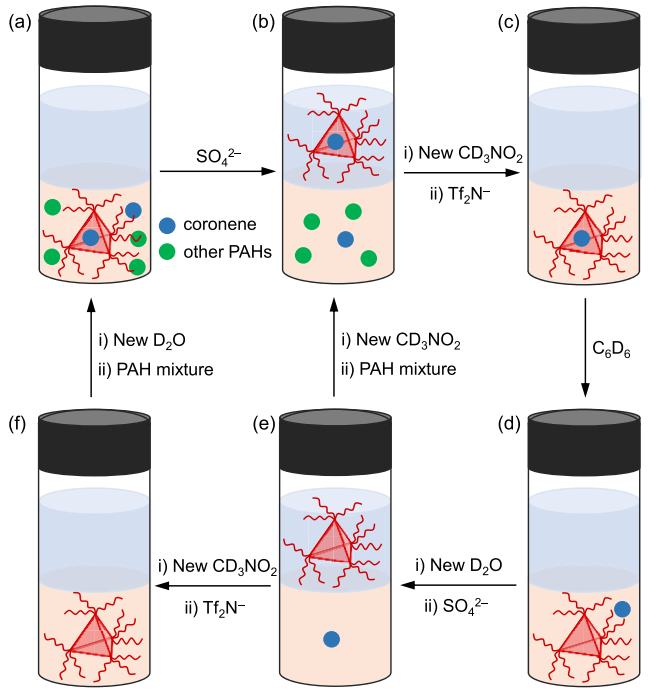

Figure 4. Selective separation and recovery of coronene from a mixture of other PAHs including anthracene, phenanthrene, pyrene, chrysene, triphenylene, perylene, and corannulene. All upper layers in these schematic vials are D_2O, and the lower layers are CD_3NO_2. (a) Cage **1** took up coronene selectively in CD_3NO_2 (0.090 mM **1**; 0.33 mM coronene, and 0.090 mM of each of the other PAHs) and (b) transferred to the aqueous layer together with its coronene cargo after the addition of SO_4^{2-}; (c) replacement of the CD_3NO_2 layer and addition of Tf_2N^- drove the complex into CD_3NO_2. (d) Cage **1** discharged the coronene cargo upon addition of C_6D_6, and the released coronene (e) was separated by transferring empty **1** to D_2O upon addition of SO_4^{2-}. (f) Cage **1** was recovered in fresh CD_3NO_2 following the addition of Tf_2N^-. Free **1** paired with SO_4^{2-} in D_2O could also directly extract coronene from a new mixture of PAHs in CD_3NO_2 (e→b).

■ ASSOCIATED CONTENT

Supporting Information

The Supporting Information is available free of charge on the ACS Publications website at DOI: 10.1021/jacs.9b10741.

Complete experimental details (PDF)

■ AUTHOR INFORMATION

Corresponding Author

*jrn34@cam.ac.uk

ORCID

Jonathan R. Nitschke: 0000-0002-4060-5122

Notes

The authors declare no competing financial interest.

■ ACKNOWLEDGMENTS

This work was supported by the European Research Council (695009) and the UK Engineering and Physical Sciences Research Council (EPSRC EP/P027067/1). The authors

DOI: 10.1021/jacs.9b10741
J. Am. Chem. Soc. 2019, 141, 18949–18953

thank the Dept. of Chemistry NMR facility, Univ. of Cambridge, for performing some NMR experiments, and the EPSRC UK National Mass Spectrometry Facility at Swansea Univ. for performing high-resolution mass spectrometry. D.Z. acknowledges a Herchel Smith Research Fellowship from the Univ. of Cambridge.

REFERENCES

(1) Harvey, R. G. *Polycyclic aromatic hydrocarbons;* Wiley-VCH: New York, 1997.
(2) Bostrom, C. E.; Gerde, P.; Hanberg, A.; Jernstrom, B.; Johansson, C.; Kyrklund, T.; Rannug, A.; Tornqvist, M.; Victorin, K.; Westerholm, R. Cancer risk assessment, indicators, and guidelines for polycyclic aromatic hydrocarbons in the ambient air. *Environ. Health Perspect.* **2002**, *110*, 451−488.
(3) Narita, A.; Wang, X. Y.; Feng, X.; Mullen, K. New advances in nanographene chemistry. *Chem. Soc. Rev.* **2015**, *44*, 6616−6643.
(4) Origuchi, S.; Kishimoto, M.; Yoshizawa, M.; Yoshimoto, S. A supramolecular approach to the preparation of nanographene adlayers using water-soluble molecular capsules. *Angew. Chem., Int. Ed.* **2018**, *57*, 15481−15485.
(5) Frischmann, P. D.; MacLachlan, M. J. Metallocavitands: an emerging class of functional multimetallic host molecules. *Chem. Soc. Rev.* **2013**, *42*, 871−890.
(6) Diaz-Moscoso, A.; Ballester, P. Light-responsive molecular containers. *Chem. Commun.* **2017**, *53*, 4635−4652.
(7) Zhang, Z.; Kim, D. S.; Lin, C. Y.; Zhang, H.; Lammer, A. D.; Lynch, V. M.; Popov, I.; Miljanic, O. S.; Anslyn, E. V.; Sessler, J. L. Expanded porphyrin-anion supramolecular assemblies: environmentally responsive sensors for organic solvents and anions. *J. Am. Chem. Soc.* **2015**, *137*, 7769−7774.
(8) Wang, Q. Q.; Day, V. W.; Bowman-James, K. Chemistry and structure of a host-guest relationship: the power of NMR and X-ray diffraction in tandem. *J. Am. Chem. Soc.* **2013**, *135*, 392−399.
(9) Jiang, B.; Wang, W.; Zhang, Y.; Lu, Y.; Zhang, C. W.; Yin, G. Q.; Zhao, X. L.; Xu, L.; Tan, H.; Li, X.; Jin, G. X.; Yang, H. B. Construction of π-surface-metalated pillar[5]arenes which bind anions via anion-π interactions. *Angew. Chem., Int. Ed.* **2017**, *56*, 14438−14442.
(10) Wu, X.; Wang, P.; Turner, P.; Lewis, W.; Catal, O.; Thomas, D. S.; Gale, P. A. Tetraurea macrocycles: aggregation-driven binding of chloride in aqueous solutions. *Chem.* **2019**, *5*, 1210−1222.
(11) Dube, H.; Ajami, D.; Rebek, J., Jr. Photochemical control of reversible encapsulation. *Angew. Chem., Int. Ed.* **2010**, *49*, 3192−3195.
(12) Jiao, Y.; Tang, B.; Zhang, Y.; Xu, J. F.; Wang, Z.; Zhang, X. Highly efficient supramolecular catalysis by endowing the reaction intermediate with adaptive reactivity. *Angew. Chem., Int. Ed.* **2018**, *57*, 6077−6081.
(13) Wang, K.; Cai, X.; Yao, W.; Tang, D.; Kataria, R.; Ashbaugh, H. S.; Byers, L. D.; Gibb, B. C. Electrostatic control of macrocyclization reactions within nanospaces. *J. Am. Chem. Soc.* **2019**, *141*, 6740−6747.
(14) Zhiquan, L.; Xie, H.; Border, S. E.; Gallucci, J.; Pavlovic, R. Z.; Badjic, J. D. A stimuli-responsive molecular capsule with switchable dynamics, chirality, and encapsulation characteristics. *J. Am. Chem. Soc.* **2018**, *140*, 11091−11100.
(15) Gropp, C.; Quigley, B. L.; Diederich, F. Molecular recognition with resorcin[4]arene cavitands: switching, halogen-bonded capsules, and enantioselective complexation. *J. Am. Chem. Soc.* **2018**, *140*, 2705−2717.
(16) Barnes, J. C.; Juricek, M.; Strutt, N. L.; Frasconi, M.; Sampath, S.; Giesener, M. A.; McGrier, P. L.; Bruns, C. J.; Stern, C. L.; Sarjeant, A. A.; Stoddart, J. F. ExBox: a polycyclic aromatic hydrocarbon scavenger. *J. Am. Chem. Soc.* **2013**, *135*, 183−192.
(17) Ibanez, S.; Peris, E. A rigid trigonal-prismatic hexagold metallocage that behaves as a coronene trap. *Angew. Chem., Int. Ed.* **2019**, *58*, 6693−6697.
(18) Alvarino, C.; Pia, E.; Garcia, M. D.; Blanco, V.; Fernandez, A.; Peinador, C.; Quintela, J. M. Dimensional matching of polycyclic aromatics with rectangular metallacycles: insertion modes determined by [C-H···π] interactions. *Chem. - Eur. J.* **2013**, *19*, 15329−15335.
(19) Wu, G.; Wang, C. Y.; Jiao, T.; Zhu, H.; Huang, F.; Li, H. Controllable self-assembly of macrocycles in water for isolating aromatic hydrocarbon isomers. *J. Am. Chem. Soc.* **2018**, *140*, 5955−5961.
(20) Peinador, C.; Pia, E.; Blanco, V.; Garcia, M. D.; Quintela, J. M. Complexation of pyrene in aqueous solution with a self-assembled palladium metallocycle. *Org. Lett.* **2010**, *12*, 1380−1383.
(21) Samanta, J.; Natarajan, R. Cofacial organic click cage to intercalate polycyclic aromatic hydrocarbons. *Org. Lett.* **2016**, *18*, 3394−3397.
(22) Dale, E. J.; Vermeulen, N. A.; Thomas, A. A.; Barnes, J. C.; Juricek, M.; Blackburn, A. K.; Strutt, N. L.; Sarjeant, A. A.; Stern, C. L.; Denmark, S. E.; Stoddart, J. F. ExCage. *J. Am. Chem. Soc.* **2014**, *136*, 10669−10682.
(23) Jie, K.; Zhou, Y.; Li, E.; Huang, F. Nonporous adaptive crystals of pillararenes. *Acc. Chem. Res.* **2018**, *51*, 2064−2072.
(24) Hasell, T.; Cooper, A. I. Porous organic cages: soluble, modular and molecular pores. *Nat. Rev. Mater.* **2016**, *1*, 16053.
(25) Zhou, Y.; Jie, K.; Zhao, R.; Huang, F. *Cis-trans* selectivity of haloalkene isomers in nonporous adaptive pillararene crystals. *J. Am. Chem. Soc.* **2019**, *141*, 11847−11851.
(26) Jie, K.; Zhou, Y.; Li, E.; Zhao, R.; Huang, F. Separation of aromatics/cyclic aliphatics by nonporous adaptive pillararene crystals. *Angew. Chem., Int. Ed.* **2018**, *57*, 12845−12849.
(27) Mitra, T.; Jelfs, K. E.; Schmidtmann, M.; Ahmed, A.; Chong, S. Y.; Adams, D. J.; Cooper, A. I. Molecular shape sorting using molecular organic cages. *Nat. Chem.* **2013**, *5*, 276−281.
(28) Chen, L.; Reiss, P. S.; Chong, S. Y.; Holden, D.; Jelfs, K. E.; Hasell, T.; Little, M. A.; Kewley, A.; Briggs, M. E.; Stephenson, A.; Thomas, K. M.; Armstrong, J. A.; Bell, J.; Busto, J.; Noel, R.; Liu, J.; Strachan, D. M.; Thallapally, P. K.; Cooper, A. I. Separation of rare gases and chiral molecules by selective binding in porous organic cages. *Nat. Mater.* **2014**, *13*, 954−960.
(29) Zhang, S. Y.; Kochovski, Z.; Lee, H. C.; Lu, Y.; Zhang, H.; Zhang, J.; Sun, J. K.; Yuan, J. Ionic organic cage-encapsulating phase-transferable metal clusters. *Chem. Sci.* **2019**, *10*, 1450−1456.
(30) Ryan, T. J.; Lecollinet, G.; Velasco, T.; Davis, A. P. Phase transfer of monosaccharides through noncovalent interactions: selective extraction of glucose by a lipophilic cage receptor. *Proc. Natl. Acad. Sci. U. S. A.* **2002**, *99*, 4863−4866.
(31) Jiang, H.; O'Neil, E. J.; Divittorio, K. M.; Smith, B. D. Anion-mediated phase transfer of Zinc(II)-coordinated tyrosine derivatives. *Org. Lett.* **2005**, *7*, 3013−3016.
(32) Lin, Q.; Yun, H. J.; Liu, W.; Song, H. J.; Makarov, N. S.; Isaienko, O.; Nakotte, T.; Chen, G.; Luo, H.; Klimov, V. I.; Pietryga, J. M. Phase-transfer ligand exchange of lead chalcogenide quantum dots for direct deposition of thick, highly conductive films. *J. Am. Chem. Soc.* **2017**, *139*, 6644−6653.
(33) Ghosh, S. K.; Ojeda, A. S.; Guerrero-Leal, J.; Bhuvanesh, N.; Gladysz, J. A. New media for classical coordination chemistry: phase transfer of Werner and related polycations into highly nonpolar fluorous solvents. *Inorg. Chem.* **2013**, *52*, 9369−9378.
(34) Wei, G. T.; Yang, Z.; Lee, C. Y.; Yang, H. Y.; Wang, C. R. Aqueous-organic phase transfer of gold nanoparticles and gold nanorods using an ionic liquid. *J. Am. Chem. Soc.* **2004**, *126*, 5036−5037.
(35) Yuan, X.; Luo, Z.; Zhang, Q.; Zhang, X.; Zheng, Y.; Lee, J. Y.; Xie, J. Synthesis of highly fluorescent metal (Ag, Au, Pt, and Cu) nanoclusters by electrostatically induced reversible phase transfer. *ACS Nano* **2011**, *5*, 8800−8808.
(36) Han, M.; Michel, R.; He, B.; Chen, Y. S.; Stalke, D.; John, M.; Clever, G. H. Light-triggered guest uptake and release by a photochromic coordination cage. *Angew. Chem., Int. Ed.* **2013**, *52*, 1319−1323.

DOI: 10.1021/jacs.9b10741
J. Am. Chem. Soc. 2019, 141, 18949−18953

(37) Custelcean, R. Anion encapsulation and dynamics in self-assembled coordination cages. *Chem. Soc. Rev.* **2014**, *43*, 1813−1824.
(38) Preston, D.; Sutton, J. J.; Gordon, K. C.; Crowley, J. D. A nona-nuclear heterometallic Pd_3Pt_6 "donut"-shaped cage: molecular recognition and photocatalysis. *Angew. Chem., Int. Ed.* **2018**, *57*, 8659−8663.
(39) Cullen, W.; Turega, S.; Hunter, C. A.; Ward, M. D. pH-dependent binding of guests in the cavity of a polyhedral coordination cage: reversible uptake and release of drug molecules. *Chem. Sci.* **2015**, *6*, 625−631.
(40) Holloway, L. R.; Bogie, P. M.; Lyon, Y.; Ngai, C.; Miller, T. F.; Julian, R. R.; Hooley, R. J. Tandem reactivity of a self-assembled cage catalyst with endohedral acid groups. *J. Am. Chem. Soc.* **2018**, *140*, 8078−8081.
(41) Bender, T. A.; Morimoto, M.; Bergman, R. G.; Raymond, K. N.; Toste, F. D. Supramolecular host-selective activation of iodoarenes by encapsulated organometallics. *J. Am. Chem. Soc.* **2019**, *141*, 1701−1706.
(42) Yan, X.; Wei, P.; Liu, Y.; Wang, M.; Chen, C.; Zhao, J.; Li, G.; Saha, M. L.; Zhou, Z.; An, Z.; Li, X.; Stang, P. J. *Endo*- and *exo*-functionalized tetraphenylethylene $M_{12}L_{24}$ nanospheres: fluorescence emission inside a confined space. *J. Am. Chem. Soc.* **2019**, *141*, 9673−9679.
(43) Hu, X.; Chai, J.; Zhang, C.; Lang, J.; Kelley, S. P.; Feng, S.; Liu, B.; Atwood, D. A.; Atwood, J. L. Biomimetic self-assembly of Co(II)-seamed hexameric metal-organic nanocapsules. *J. Am. Chem. Soc.* **2019**, *141*, 9151−9154.
(44) Takezawa, H.; Kanda, T.; Nanjo, H.; Fujita, M. Site-selective functionalization of linear diterpenoids through U-shaped folding in a confined artificial cavity. *J. Am. Chem. Soc.* **2019**, *141*, 5112−5115.
(45) Howlader, P.; Mondal, B.; Purba, P. C.; Zangrando, E.; Mukherjee, P. S. Self-assembled Pd(II) barrels as containers for transient merocyanine form and reverse thermochromism of spiropyran. *J. Am. Chem. Soc.* **2018**, *140*, 7952−7960.
(46) Mendez-Arroyo, J.; d'Aquino, A. I.; Chinen, A. B.; Manraj, Y. D.; Mirkin, C. A. Reversible and selective encapsulation of dextromethorphan and β-estradiol using an asymmetric molecular capsule assembled via the weak-link approach. *J. Am. Chem. Soc.* **2017**, *139*, 1368−1371.
(47) Yamashina, M.; Kusaba, S.; Akita, M.; Kikuchi, T.; Yoshizawa, M. Cramming versus threading of long amphiphilic oligomers into a polyaromatic capsule. *Nat. Commun.* **2018**, *9*, 4227.
(48) Zhang, X.; Dong, X.; Lu, W.; Luo, D.; Zhu, X. W.; Li, X.; Zhou, X. P.; Li, D. Fine-tuning apertures of metal-organic cages: encapsulation of carbon dioxide in solution and solid state. *J. Am. Chem. Soc.* **2019**, *141*, 11621−11627.
(49) Grommet, A. B.; Nitschke, J. R. Directed phase transfer of an $Fe^{II}_4L_4$ cage and encapsulated cargo. *J. Am. Chem. Soc.* **2017**, *139*, 2176−2179.
(50) Grommet, A. B.; Hoffman, J. B.; Percastegui, E. G.; Mosquera, J.; Howe, D. J.; Bolliger, J. L.; Nitschke, J. R. Anion exchange drives reversible phase transfer of coordination cages and their cargoes. *J. Am. Chem. Soc.* **2018**, *140*, 14770−14776.
(51) Percastegui, E. G.; Mosquera, J.; Ronson, T. K.; Plajer, A. J.; Kieffer, M.; Nitschke, J. R. Waterproof architectures through subcomponent self-assembly. *Chem. Sci.* **2019**, *10*, 2006−2018.
(52) Zhang, D.; Ronson, T. K.; Greenfield, J. L.; Brotin, T.; Berthault, P.; Leonce, E.; Zhu, J. L.; Xu, L.; Nitschke, J. R. Enantiopure $[Cs^+/Xe\subset cryptophane]\subset Fe^{II}_4L_4$ hierarchical superstructures. *J. Am. Chem. Soc.* **2019**, *141*, 8339−8345.
(53) Catti, L.; Kishida, N.; Kai, T.; Akita, M.; Yoshizawa, M. Polyaromatic nanocapsules as photoresponsive hosts in water. *Nat. Commun.* **2019**, *10*, 1948.
(54) Zhang, D.; Ronson, T. K.; Nitschke, J. R. Functional capsules via subcomponent self-assembly. *Acc. Chem. Res.* **2018**, *51*, 2423−2436.

DOI: 10.1021/jacs.9b10741
J. Am. Chem. Soc. 2019, 141, 18949−18953